Journal of
Mechanics of
Materials and Structures

NUMERICAL IMPLEMENTATION OF A CONSTITUTIVE MODEL FOR SOIL CREEP

M. A. K. M. Madurapperuma and U. G. A. Puswewala

Volume 3, Nº 10 December 2008

mathematical sciences publishers

JOURNAL OF MECHANICS OF MATERIALS AND STRUCTURES
Vol. 3, No. 10, 2008

NUMERICAL IMPLEMENTATION OF A CONSTITUTIVE MODEL FOR SOIL CREEP

M. A. K. M. MADURAPPERUMA AND U. G. A. PUSWEWALA

We discuss the numerical implementation of a creep constitutive model to facilitate the modeling of long-term soil creep. Multidimensional soil creep models are generalized from the one-dimensional soil creep model proposed by Bjerrum in 1967, which was based on field test data and was later modified for transient loading conditions by Vermeer et al. in 1998. Here this differential form of one-dimensional creep model is extended to two- and three-dimensional states of stress and strain by incorporating concepts from viscoplasticity. The devised multidimensional creep model takes into account both volumetric and deviatoric creep strain, with creep deformation of the soil defined by several material parameters. The model is incorporated as a plane strain element subroutine in a nonlinear, time-incrementing finite element program, along with iterative corrections within each time step. Numerical analyses are conducted to demonstrate soil creep by using published experimental data. The verified computer code will be a useful research tool for estimating settlements in structures founded on soils exhibiting creep.

1. Introduction

Many theories have been proposed to explain the time-dependent deformation of soils under load. Bjerrum [1967], in his study of settlement of 3000 years old deposits of Norwegian clay, proposed the concept that deformation of such soils can be decomposed into two parts: "instant compression" and "delayed compression", or soil creep. This was a departure from the view where soil is understood to undergo "primary consolidation" followed by "secondary consolidation or compression" [Terzaghi 1931]. Bjerrum's argument was that under constant load, creeping soils continue to experience strain with time, thus causing an increase of its critical pressure. The term critical pressure is used to define a specific effective pressure (preconsolidation pressure) in the classical void ratio versus log pressure graph for a soil medium [Balasubramaniam and Brenner 1981]. Thus if the soil is allowed to creep under a particular load over a long period and if the load is suddenly increased thereafter, the soil behaves as if it had been subjected to a much greater pressure than the previous maximum pressure it physically sustained.

Bjerrum gave examples of buildings founded on Norwegian clay undergoing creep settlements. Similar creep settlements can take place under other structures like roads, river embankments and dams, built on creeping media. Apart from the foundation-related problems usually considered, creep plays an important role in slope stability; gradual geometric changes due to creep and the associated reduction of strength due to the smoothening of soil particles may then lead to slope slides. The different problems that relate to soil creep have made it necessary to develop a stress-strain relation that takes two- and three-dimensional situations into account.

Keywords: constitutive model, finite element analysis, soil creep, numerical simulation, soil-structure interaction.

As mentioned, Bjerrum's original creep model was a comprehensive one-dimensional model based on the behavior of Norwegian clays with a sedimentation history of 3000 years. It was based on an expression for creep rate for constant effective stress; it was modified for transient loading conditions by Vermeer et al. [1998] and later generalized to three dimensions [Vermeer and Neher 1999]. However, the generalized constitutive model is not in a form that can be implemented in finite element formulation for numerical simulation of soil creep. Adachi and Okano [1974] proposed a rate-formulated elastoviscoplastic constitutive model, later generalized in [Adachi and Oka 1982] based on the overstress type viscoplastic theory. However, this model has not been verified for predicting the time-dependent long-term behavior of soft soils. [Borja and Kavazvjian 1985] proposed a constitutive model to describe time dependent elasto-plastic strains based on Bjerrum's concept. The validity of this model was not properly verified through realistic experimental approaches and its long-term predictive capability has not been comprehensively reported in the literature.

On the other hand, numerical implementation by using the finite element method has taken into account creep of soil using nonlinear constitutive equations; see, for example, [Iizuka and Ohta 1987; Stolle et al. 1997; Brinkgreve 2002]. A detailed description of numerical implementation of advanced constitutive models is presented in [Stolle et al. 1997; Wheeler et al. 2003]. The long term prediction of soft soil settlement is dependent on the constitutive model that describes the soil creep behavior and the finite element formulation which involves solution algorithms, iteration schemes, time increments and numerical stability. Therefore, a simple creep model that could describe all aspects of actual field behavior to sufficient accuracy would be highly useful and suitable for practical applications. Based on an extensive literature review, we found the constitutive model proposed by Vermeer et al. [1998] based on Bjerrum's one-dimensional model to be one of the most appropriate for generalization and numerical implementation. Its ability to predicting long-term time-dependent soil behavior and the evaluation of model parameters through conventional tests in the laboratory are the main reasons to select this model.

Here we extend the model of [Vermeer et al. 1998] to multidimensional state of stress and strain by incorporating concepts of viscoplasticity. A nonlinear, time incrementing finite element program, with iterative corrections within each time step, developed earlier to model creep in geomaterials [Puswewala et al. 1992], is modified to incorporate the present model as an element subroutine under conditions of plane strain. Numerical analyses are conducted for two soil-structure interaction problems by using this program and published experimental data to demonstrate the creep behavior of soils predicted by the model.

2. The differential form of one-dimensional creep model

In his Rankine Lecture, Bjerrum [1967] described the compression of clays exhibiting creep under constant effective stress. Building on this work, Garlanger [1972] proposed a creep equation of the form

$$e = e_c - C_\alpha \log \frac{\tau_c + t'}{\tau_c}, \tag{1}$$

where e is the void ratio, e_c is the void ratio at the end of consolidation, $t' > 0$ is the effective creep time, and C_α is the slope of the e versus log time curve. The time scale parameter τ_c depends on the history

of compression and the geometry of the sample. Janbu [1969] developed a construction for evaluating τ_c from experimental data.

This expression was later modified by Butterfield [1979] to fit into the framework of critical state soil mechanics. He introduced the concept of logarithmic strain. The expression of the total volumetric strain, ε_v, is

$$\varepsilon_v = \varepsilon_v^c + \mu^* \ln \frac{\tau_c + t'}{\tau_c}, \tag{2}$$

where the deformation during primary consolidation is given by ε_v^c and consists of the elastic settlement and a part of the delayed settlement, following Bjerrum. The modified secondary compression index μ^* describes the secondary compression per logarithmic time increment. Equation (2) can be rewritten by including the components of ε_v^c as

$$\varepsilon_v = \varepsilon_v^c + \varepsilon_v^{cr} = k^* \ln \frac{\sigma'}{\sigma_0'} + (\lambda^* - k^*) \ln \frac{\sigma_{pc}'}{\sigma_{p0}'} + \mu^* \ln \frac{\tau_c + t'}{\tau_c}, \tag{3}$$

where

- ε_v is the total volumetric strain due to an increase in mean effective stress from σ_0' to σ' in a time period of $(\tau_c + t')$,
- σ_{p0}' and σ_{pc}' represent the preconsolidation pressure corresponding to before-loading state and end-of-consolidation state respectively,
- k^*, λ^*, μ^* are the Modified Clam Clay Model parameters [Roscoe and Burland 1968], called respectively the (modified) swelling index, compression index and creep index, and having the values

$$\lambda^* = \frac{C_c}{2.3(1+e_0)}, \quad k^* \approx \frac{3}{2.3} \frac{(1-\nu)}{(1+\nu)} \frac{C_r}{1+e_0}, \quad \mu^* = \frac{C_\alpha}{2.3(1+e_0)}, \tag{4}$$

  where C_r is the slope on an e versus log σ' diagram of the compression line from σ_0' to σ_c', C_c is the slope of the instant line, C_α is the slope of the e versus log time curve, ν is the Poisson's ratio, e_0 is the initial void ratio and σ_c' is the preconsolidation pressure [Vermeer et al. 1998].

Equation (3) is valid for a constant mean effective stress, but for transient or continuous loading problems it is necessary to formulate a constitutive law in differential form. Moreover there is still the question of how to express the time scale parameter τ_c analytically. By adopting Bjerrum's concept that the secondary compression increases the critical pressure (preconsolidation pressure), by eliminating σ_{pc}' and τ_c from (3), Vermeer et al. proposed a differential form of expression that accounts for creep of soft soil, of the form

$$\dot{\varepsilon}_v = \dot{\varepsilon}_v^e + \dot{\varepsilon}_v^c = \kappa^* \frac{\dot{\sigma}'}{\sigma'} + \frac{\mu^*}{\tau} \left(\frac{\sigma'}{\sigma_p'} \right)^{(\lambda^* - \kappa^*)/\mu^*} \quad \text{in which } \sigma_p' = \sigma_{p0}' \exp \frac{\varepsilon_v^c}{\lambda^* - \kappa^*}, \tag{5}$$

where the parameter τ, which is not the same as τ_c, is introduced to provide a time scale and an additional degree of freedom in the soil creep model. For example, in the conventional consolidation test each load is kept for one day and at the end of the day the isotropic consolidation line with $\sigma_p' = \sigma'$ is obtained (overconsolidation ratio = 1). Therefore, in the case of conventional consolidation test the time scale parameter τ can be taken as precisely 1 day. The quantity ε_v^c is the accumulated volumetric creep strain.

3. Generalization of the one-dimensional model to three dimensions

The expression for volumetric creep strain rate ($\dot{\varepsilon}_v^c$) in (5) is extended for a general state of stress and strain. Well-known stress invariant quantities are adopted for pressure p and deviatoric stress q as $p = \sigma_{\text{oct}}$ and $q = 3\tau_{\text{oct}}/\sqrt{2}$, where σ_{oct} and τ_{oct} are the octahedral normal stress and octahedral shear stress. In terms of the principal stresses $\sigma_1,\ \sigma_2,\ \sigma_3$, the pressure p and the deviatoric stress q can be expressed as

$$p = \tfrac{1}{3}\,(\sigma_1 + \sigma_2 + \sigma_3) \quad \text{and} \quad q = \sqrt{\tfrac{1}{2}\big((\sigma_1 - \sigma_2)^2 + (\sigma_2 - \sigma_3)^2 + (\sigma_3 - \sigma_1)\big)^2}. \tag{6}$$

The extension of (6) to a state of general stress and strain yields

$$p = \tfrac{1}{3}\,(\sigma_{ii}) \quad \text{and} \quad q = \sqrt{\tfrac{3}{2}\,(s_{ij}s_{ij})}, \tag{7}$$

where summation is implied over the indices $i, j = 1, 2, 3$ and s_{ij} denotes the deviatoric stress tensor in terms of multidimensional states of stress quantities as

$$s_{ij} = \sigma_{ij} - \tfrac{1}{3}\sigma_{ii}\delta_{ij}, \tag{8}$$

where δ_{ij} is Kronecker's delta. The invariants p and q [Roscoe and Burland 1968] can be used to define a new stress measure [Vermeer and Neher 1999]

$$p^{\text{eq}} = p + \frac{q^2}{M^2 p}, \tag{9}$$

called *equivalent pressure* and having the dimension of pressure. The soil parameter M represents the slope of the critical state line and can be computed by using the critical state friction angle (ϕ_{cs}) as

$$M = \frac{6\,\sin\phi_{\text{cs}}}{3 - \sin\phi_{\text{cs}}}. \tag{10}$$

(see [Vermeer et al. 1998]). For principal stress quantities yield function is defined as

$$f = p^{\text{eq}} - p_p^{\text{eq}}, \tag{11}$$

where p_p^{eq} is the apparent equivalent preconsolidation pressure. The yield function f in (11) can be described as ellipses in p-q space when the principal stress quantities are used to calculate p and q in (6). The equivalent pressure p^{eq} is constant on ellipses and the peaks of the ellipses are located on the critical state line which is given by the model of [Roscoe and Burland 1968] in p-q space.

Together with p and q in (7), the equivalent pressure p^{eq} in (9) leads to

$$p^{\text{eq}} = \tfrac{1}{3}\sigma_{ii} + \frac{9\,s_{ij}s_{ij}}{2\,M^2\sigma_{ii}}. \tag{12}$$

By considering the volumetric creep strain rate part ($\dot{\varepsilon}_v^c$) in (5) and introducing the new equivalent pressure p^{eq} and the apparent equivalent preconsolidation pressure p_p^{eq} the expression for volumetric creep strain rate can be written as

$$\dot{\varepsilon}_v^c = \frac{\mu^*}{\tau}\left(\frac{p^{\text{eq}}}{p_p^{\text{eq}}}\right)^{(\lambda^* - \kappa^*)/\mu^*}, \quad \text{with } p_p^{\text{eq}} = p_{p0}^{\text{eq}} \exp\frac{\varepsilon_v^c(t)}{\lambda^* - \kappa^*}, \tag{13}$$

where $\varepsilon_v^c(t)$denotes the accumulated volumetric creep up to the current time t. The coefficient of lateral earth pressure K_0^{NC} is used to estimate the initial value of equivalent preconsolidation pressure p_{p0}^{eq} using initial preconsolidation pressure σ_{p0} as given in [Vermeer and Neher 1999; Vermeer et al. 1998].

4. Formulation of the soil creep problem

The basic concept used here is that the total strain vector consists of an elastic strain component and a creep strain component:

$$\boldsymbol{\varepsilon}(t) = \boldsymbol{\varepsilon}^e(t) + \boldsymbol{\varepsilon}^c(t), \tag{14}$$

where $\boldsymbol{\varepsilon}(t)$ is the current total strain vector, $\boldsymbol{\varepsilon}^e(t)$ the current elastic strain vector, $\boldsymbol{\varepsilon}^c(t)$ the current creep strain vector, and t denotes the current time. The elastic strain component can be related to the stress vector $\boldsymbol{\sigma}(t)$ through the use of a constitutive matrix $\boldsymbol{D}$ as

$$\boldsymbol{\varepsilon}^e(t) = \boldsymbol{D}^{-1}\boldsymbol{\sigma}(t). \tag{15}$$

In the present analysis $\boldsymbol{D}$ is composed of Young's modulus E and Poisson's ratio ν, which implies that the elastic strain is related to stress according to isotropic linear elasticity. In order to introduce general creep strain, one can adopt the view that creep strain is simply a time-dependent plastic strain. Then it is logical to assume a flow rule for the creep rate component and equivalent pressure p^{eq} is introduced as the plastic potential function [Vermeer et al. 1998]. Assuming the same yield function as in (11) the total strain rate can then be obtained as

$$\dot{\boldsymbol{\varepsilon}}(t) = \boldsymbol{D}^{-1}\dot{\boldsymbol{\sigma}}(t) + \lambda\frac{\partial p^{\text{eq}}}{\partial\boldsymbol{\sigma}(t)}, \tag{16}$$

where the plastic multiplier λ can be eliminated from (16) by adopting the concept that the creep strain rate is proportional to partial derivative of the plastic potential function with respect to the corresponding stress component, i.e.,

$$\lambda = \frac{\dot{\boldsymbol{\varepsilon}}_v^c}{\boldsymbol{\alpha}}, \tag{17}$$

where λ can be evaluated for multidimensional situation as

$$\dot{\boldsymbol{\varepsilon}}_v^c = \dot{\varepsilon}_{11}^c + \dot{\varepsilon}_{22}^c + \dot{\varepsilon}_{33}^c \quad \text{and} \quad \boldsymbol{\alpha} = \left(\frac{\partial p^{\text{eq}}}{\partial\sigma_{11}} + \frac{\partial p^{\text{eq}}}{\partial\sigma_{22}} + \frac{\partial p^{\text{eq}}}{\partial\sigma_{33}}\right). \tag{18}$$

Equations (14)–(18) yield

$$\dot{\boldsymbol{\varepsilon}}^c(t) = \frac{\dot{\boldsymbol{\varepsilon}}_v^c}{\alpha}\frac{\partial p^{\text{eq}}}{\partial\boldsymbol{\sigma}(t)}. \tag{19}$$

By combining(13) and (19) we obtain

$$\dot{\boldsymbol{\varepsilon}}^c(t) = \frac{1}{\alpha}\frac{\mu^*}{\tau}\left(\frac{p^{\text{eq}}}{p_p^{\text{eq}}}\right)^{(\lambda^*-\kappa^*)/\mu^*}\frac{\partial p^{\text{eq}}}{\partial\boldsymbol{\sigma}(t)}, \quad \text{with } p_p^{\text{eq}} = p_{p0}^{\text{eq}}\exp\frac{\varepsilon_v^c(t)}{\lambda^*-\kappa^*}. \tag{20}$$

Note that the subscript 0 is used in the equations to denote initial conditions and that $\varepsilon_v^c = 0$ for time $t = 0$. The derivative quantities of p^{eq} and the components of strain rate vector $\dot{\boldsymbol{\varepsilon}}^c$ are given in the Online Supplement.

5. Finite element algorithm for creep model

A finite element algorithm was developed for the purpose of incorporating the devised creep model under plane strain conditions, based on [Puswewala et al. 1992]. At any point within a material domain of volume V and surface S, discretized by finite elements, the displacement vector field will be denoted by $\boldsymbol{u}$, the strain vector by $\boldsymbol{\varepsilon}$, and the stress vector by $\boldsymbol{\sigma}$. From the principle of virtual work, equilibrium of the material domain at the time t_k, which is reached after the accumulation of k time steps starting from $t = 0$, can be expressed as

$$\int_v \boldsymbol{B}^T \boldsymbol{\sigma}_k dv + \boldsymbol{f}_k = \boldsymbol{0}, \tag{21}$$

where $\boldsymbol{f}_k$ is the known force vector consisting of body forces and surface traction forces. Vectors $\boldsymbol{B}$, $\boldsymbol{u}$, $\boldsymbol{\varepsilon}$ and the nodal displacement vector $\boldsymbol{a}$ hold the following relationships, i.e.,

$$\boldsymbol{\varepsilon} = \boldsymbol{L}\boldsymbol{u}, \quad \boldsymbol{u} = \boldsymbol{N}\boldsymbol{a} \quad \text{and} \quad \boldsymbol{\varepsilon} = \boldsymbol{L}\boldsymbol{N}\boldsymbol{a} = \boldsymbol{B}\boldsymbol{a}, \tag{22}$$

where $\boldsymbol{N}$ is the shape function matrix and $\boldsymbol{L}$ is a differential operator matrix. It is necessary to evaluate $\boldsymbol{a}_{k+1}$ and $\boldsymbol{\sigma}_{k+1}$ at the end of the next time interval Δt_k, provided $\boldsymbol{\varepsilon}_k$, $\boldsymbol{a}_k$and $\boldsymbol{\sigma}_k$ at the time t_k are known. In order to evaluate the accumulated volumetric creep strain (ε_v^c) at the time t_k, Equations (14) and (15) are used since $\boldsymbol{\varepsilon}_k$, $\boldsymbol{D}^{-1}$and $\boldsymbol{\sigma}_k$ are known quantities at the time t_k. Together with (14), (15) and (22), the expression for the difference between the stress vectors $\boldsymbol{\sigma}_{k+1}$ and $\boldsymbol{\sigma}_k$ can be obtained as

$$\boldsymbol{\psi}_{k+1} \equiv \boldsymbol{\sigma}_{k+1} - \boldsymbol{\sigma}_k - \boldsymbol{D}\boldsymbol{B}\{\boldsymbol{a}_{k+1} - \boldsymbol{a}_k\} + \boldsymbol{D}\Delta t_k \boldsymbol{\beta}(\boldsymbol{\sigma}_{k+\theta}) = \boldsymbol{0}. \tag{23}$$

In the above, the following relationship has been used

$$\boldsymbol{\varepsilon}^c_{k+1} - \boldsymbol{\varepsilon}^c_k = \boldsymbol{\beta}(\boldsymbol{\sigma}_{k+\theta})\Delta t_k, \tag{24}$$

where $\boldsymbol{\beta}$ denotes the strain rate vector given by (20), and

$$\boldsymbol{\sigma}_{k+\theta} = (1-\theta)\boldsymbol{\sigma}_k + \theta\boldsymbol{\sigma}_{k+1}, \quad \text{where} \quad 0 \leqslant \theta \leqslant 1. \tag{25}$$

For $\theta \geqslant \frac{1}{2}$ (i.e., to have a unconditionally stable scheme), Newton–Raphson procedure is used to iterate within the time interval Δt_k for the unknowns $\boldsymbol{\sigma}_{k+1}$ and $\boldsymbol{a}_{k+1}$. The iterate number is denoted by a superscript numeral. After successive iterations, the iteration cycle n can be reached, while the convergence criterion may not yet be satisfied. At this point, (21) and (23) can be written using the appropriate current stress and displacement values, but these expressions would now not reduce to zero since convergence has not yet been achieved. Using the curtailed Taylor expansion on the latter expressions, the following two equations are obtained to yield the unknown incremental corrections $\Delta\boldsymbol{\sigma}^n_{k+1}$ and $\Delta\boldsymbol{a}^n_{k+1}$ upon solution (this is the $(n+1)$-th iterate):

$$\Delta\boldsymbol{\sigma}^n_{k+1} = \bar{\boldsymbol{D}}^n \left[\boldsymbol{B}\left(\Delta\boldsymbol{a}^n_{k+1} + \boldsymbol{a}^n_{k+1} - \boldsymbol{a}_k\right) - \boldsymbol{D}^{-1}\left(\boldsymbol{\sigma}^n_{k+1} - \boldsymbol{\sigma}_k\right) - \Delta t_k \boldsymbol{\beta}\left(\boldsymbol{\sigma}^n_{k+\theta}\right)\right], \tag{26}$$

$$\int_v \boldsymbol{B}^T \bar{\boldsymbol{D}}^n \boldsymbol{B}\ \Delta\boldsymbol{a}^n_{k+1}\, dv = \int_v \boldsymbol{B}^T \bar{\boldsymbol{D}}^n \left\{\boldsymbol{D}^{-1}\left(\boldsymbol{\sigma}^n_{k+1} - \boldsymbol{\sigma}_k\right) - \boldsymbol{B}\left(\boldsymbol{a}^n_{k+1} - \boldsymbol{a}_k\right) + \Delta t_k \boldsymbol{\beta}\left(\boldsymbol{\sigma}^n_{k+\theta}\right)\right\} dv - \int_v \boldsymbol{B}^T \boldsymbol{\sigma}^n_{k+1} dv, \tag{27}$$

where $\boldsymbol{\sigma}^n_{k+\theta}$ is obtained from (25) by replacing $\boldsymbol{\sigma}_{k+1}$ with $\boldsymbol{\sigma}^n_{k+1}$, and

$$\bar{\boldsymbol{D}}^n = \left[\boldsymbol{D}^{-1} + \Delta t_k \boldsymbol{S}^n \theta\right]^{-1}, \tag{28}$$

where the matrix

$$\boldsymbol{S}^n = \left(\frac{\partial \boldsymbol{\beta}}{\partial \boldsymbol{\sigma}}\right), \tag{29}$$

is evaluated for $\boldsymbol{\sigma}^n_{k+\theta}$. In (27) the right-hand side does not include provisions for increasing body forces. If convergence occurs at the above $(n+1)$-the iterate, we set $\boldsymbol{\sigma}_{k+1} = \boldsymbol{\sigma}^{n+1}_{k+1}$ (note that $\boldsymbol{\sigma}^{n+1}_{k+1} = \boldsymbol{\sigma}^n_{k+1} + \Delta\boldsymbol{\sigma}^n_{k+1}$) and $\boldsymbol{a}_{k+1} = \boldsymbol{a}^{n+1}_{k+1}$, and proceed to the next time step; otherwise iteration is continued. The components of the matrix $\boldsymbol{S}^n$ and the expressions for the element stiffness matrix and the stress increments are given in the Online Supplement.

There are several possibilities that can be followed for convergence study, depending on the values of θ and n (for example, $\theta \neq 0$ and $n = 1$). The value of θ used in the analysis is $\frac{1}{2}$, which guarantees the numerical stability of the algorithm. As an approximation has already been incorporated at the stage of writing (24), the iteration solution is generally curtailed after one or two cycles. Use of sufficiently small time steps would compensate for these approximations. As per the constitutive model in (20), the solution process is initiated by obtaining the instantaneous elastic deformation and stress distribution at the time of application of the initial load ($t = 0$). These displacement and stress vectors are used to obtain the incremental displacement and stress vectors during the first time interval Δt_0 by solving (26) and (27). The solution process is repeated for each time interval, until the termination of analysis. The flow diagram for FEM algorithm is given in Figure 1.

6. Numerical analysis and discussion

The sensitivity analysis of material parameters used in the model is carried out by simulating a concrete strip foundation on a soil layer. Numerical analyses were carried out by a finite element mesh composed of 40 eight-node serendipity elements representing an 8 m deep layer of soft soil underlain by a hard surface like rock (Figure 2). The simulation was done under simplified plane strain conditions, with the top of the surface subjected to a uniform load of 120 kPa applied over the strip footing. The strip footing materials were selected as concrete and the basic material properties of the soil were selected similar to Haney clay investigated by Vaid and Campanella [1977], and the corresponding material parameters are as follows:

Foundation material parameters: Young's modulus $E = 2.1 \times 10^7$ kPa; Poisson's ratio $\nu = 0.23$

Soil properties for the problem configuration in Figures 2 and 6:

$$E = 2.1 \times 10^4\,\text{kPa}, \quad \nu = 0.25, \quad \sigma_{p0} = 350\,\text{kPa}, \quad \phi_{\text{cs}} = 32.1,$$
$$\kappa^* = 0.016, \quad \lambda^* = 0.105, \quad \mu^* = 0.004 \quad \tau = 1\,\text{day} \tag{30}$$

Figure 3 shows the settlement behavior at the center of the foundation predicted by the constitutive model for different combinations of Young's modulus and Poisson's ratio. The settlement reduces when Poisson's ratio is equal to 0.45, which is as expected since incompressible behavior is represented by the case where Poisson's ratio equals 0.5. The figure shows the significant effect of parameters E and ν on the time dependent deformation of the creeping soil medium, implying that these parameters indicate the

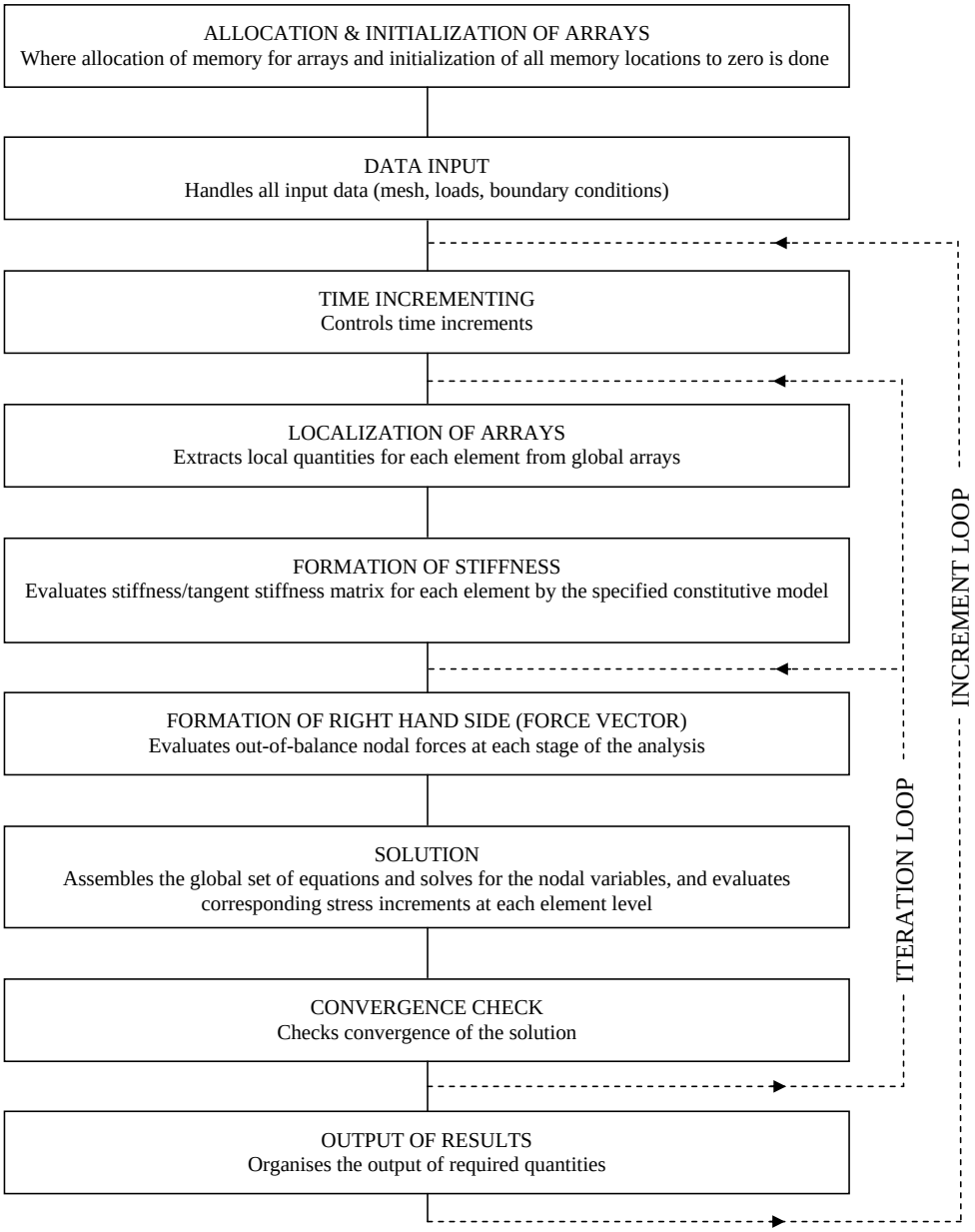

Figure 1. Flow diagram for FEM algorithm.

overall stiffness of the soil modeled as a solid continuum in this work. The effect of modified secondary compression index, μ^*, on the settlement is shown in Figure 4; the settlement with time at the center point under the surface load of 120 kN/m^2 is shown for three different values of μ^*, with all other parameters as given in (30). Figure 4 clearly indicates that the settlement increases with the increase of modified secondary compression index. The effect of preconsolidation pressure (σ_{p0}) on the settlement is shown in the Figure 5; the settlement with time at the center point under the surface load of 120 kN/m^2 is

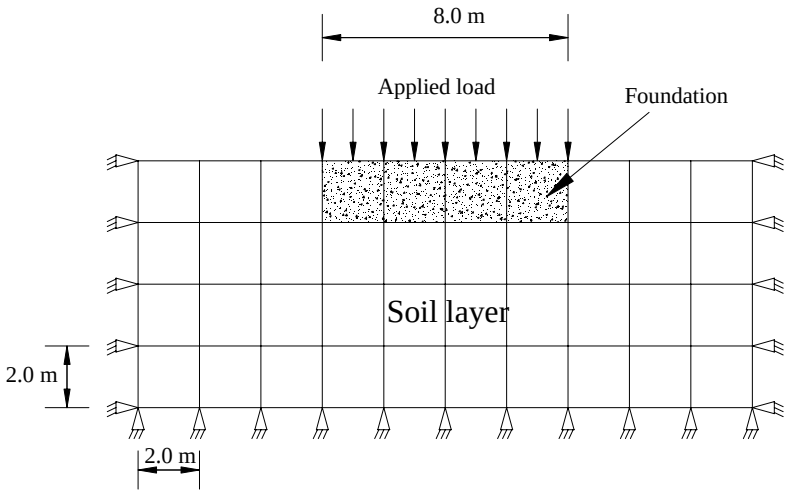

Figure 2. Finite element mesh and loading arrangement for the problem considered for sensitivity analysis.

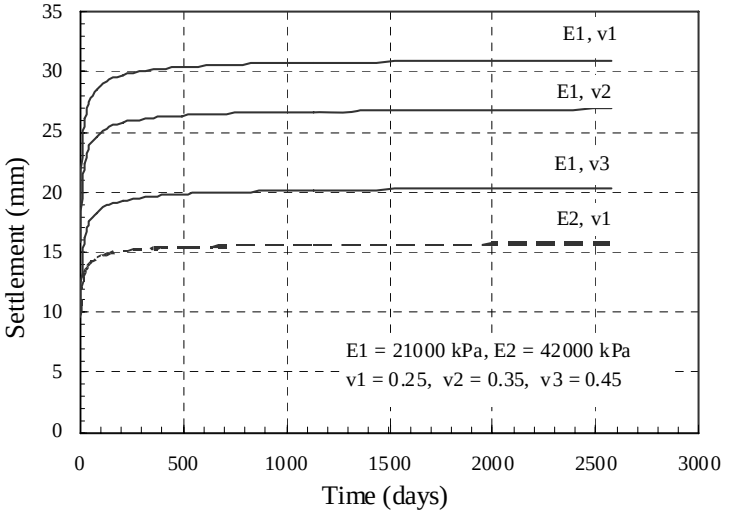

Figure 3. Settlement behavior of the center point with Young's modulus and Poisson's ratio.

shown for three different values of σ_{p0}, with all other parameters as given in (30). With the decrease of preconsolidation pressure, the figure indicates higher settlements which confirm Bjerrum's. If the preconsolidation pressure is less than the applied pressure then the settlement could be appreciable, but the problem does not work for those values due to numerical complications inherent in the model.

Another soil-structure interaction problem, where a strip footing is placed on a thick clay stratum, is considered for numerical simulation. The simulation is carried out by a finite element mesh composed of 445 eight-node serendipity elements under simplified plane strain conditions (Figure 6). Load is transferred to the soil through a wall of thickness 0.4 m on a foundation 2.4 m wide and 0.4 m high. The configuration has symmetry, and the far boundaries of the soil domain are considered at distances

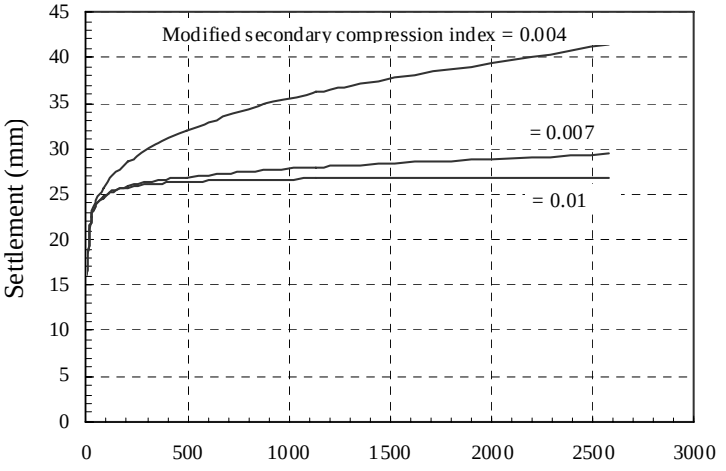

Figure 4. Settlement behavior of the center point with modified secondary compression index.

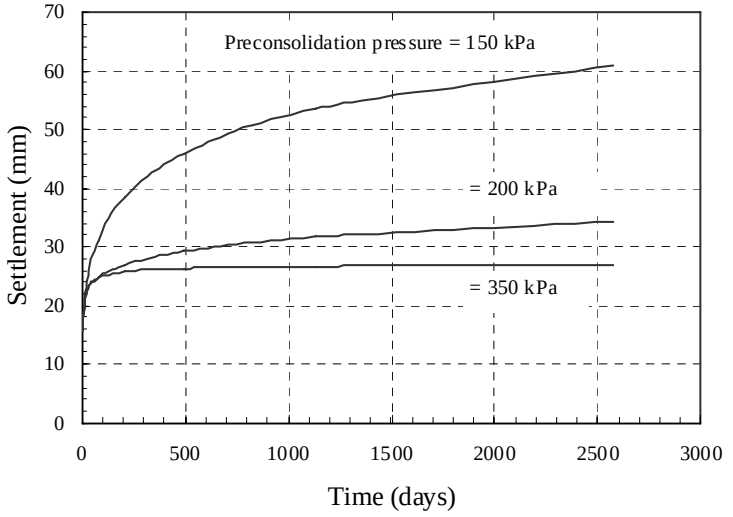

Figure 5. Settlement behavior of the center point with preconsolidation pressure.

sufficiently far from the foundation to render the boundary effects on the interaction problem insignificant. A structural load of 300 kN/m is assumed to act along the wall, equivalent to a load of 125 kPa transferred to the soil through the foundation. The wall and the footing materials were selected as concrete and the material properties of the soil are given in (30).

The problem configuration shown in Figure 6 deals with a soil-structure interaction that can often exist in the real field. By taking L as the ratio of distance to the point from the center of the loaded area to the half the total foundation width (1.2 m), the total settlement with time is shown in Figure 7 for three selected points at the foundation base level. According to this figure, the rate of settlement

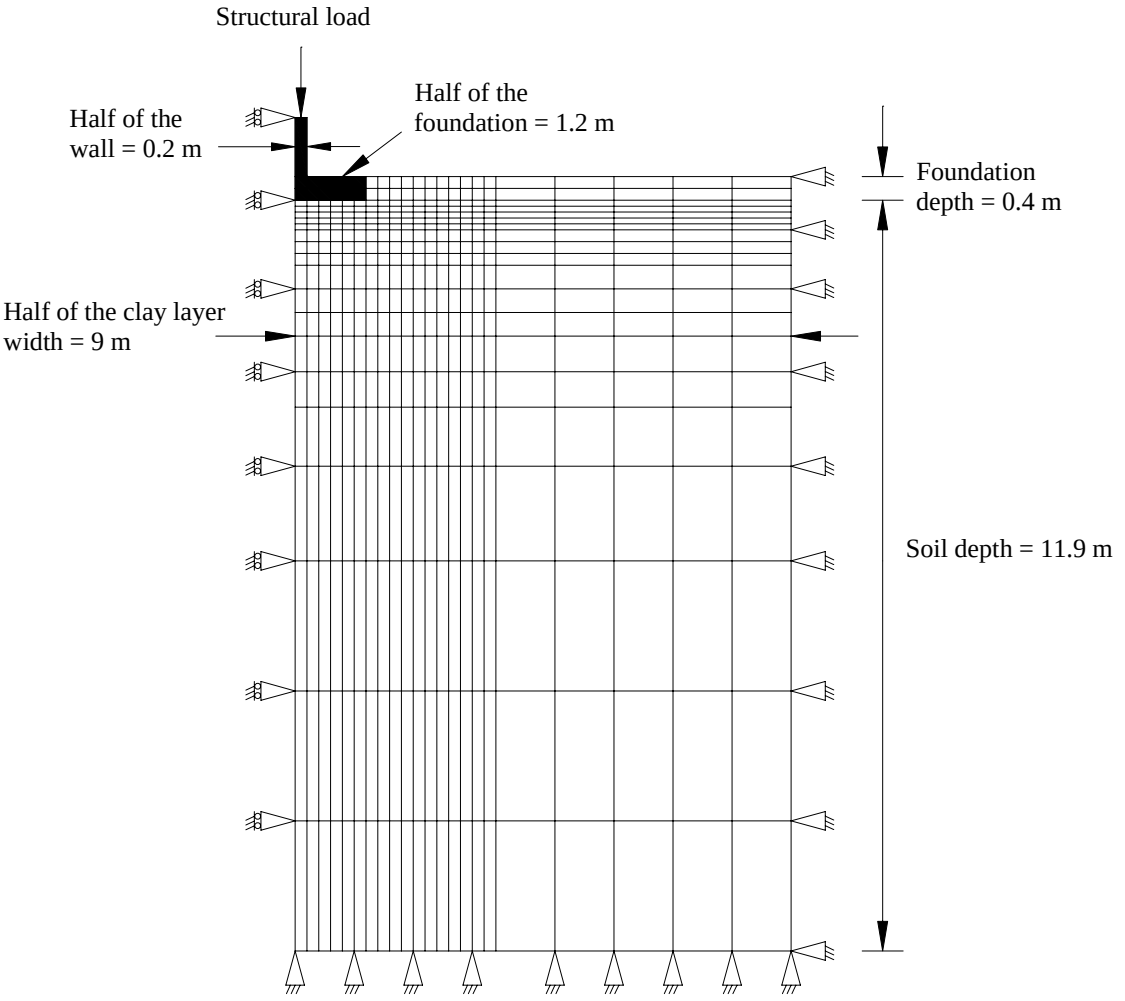

Figure 6. Finite element mesh and loading arrangement for the problem considered for numerical simulation.

decreases, whereby during the first year it has a rate of 4 mm per year while after eight years it has a rate of 1mm per year. The settlement of the foundation base with time is shown in Figure 8, which indicates that delayed settlement is several times the instant settlement. The predicted instant (elastic) settlement is about 7.5 mm and delayed settlement is about 29 mm underneath the loaded foundation after approximately eight years.

The vertical average normal stress distribution in the soil along vertical sections at distances of 0.1 m, 0.5 m, 1.1 m and 2.1 m away from the centerline with time are shown in Figures 9–12, respectively. Figures 9–11 show the time dependent variation of vertical average normal stress in the creeping material along three vertical sections underneath the loaded foundation, and indicate that stresses increase with time along the depth, towards the applied average stress at the base. This is equivalent to the geological phenomena whereby rocks undergoing creep over time reach lithostatic states of stress in the long term.

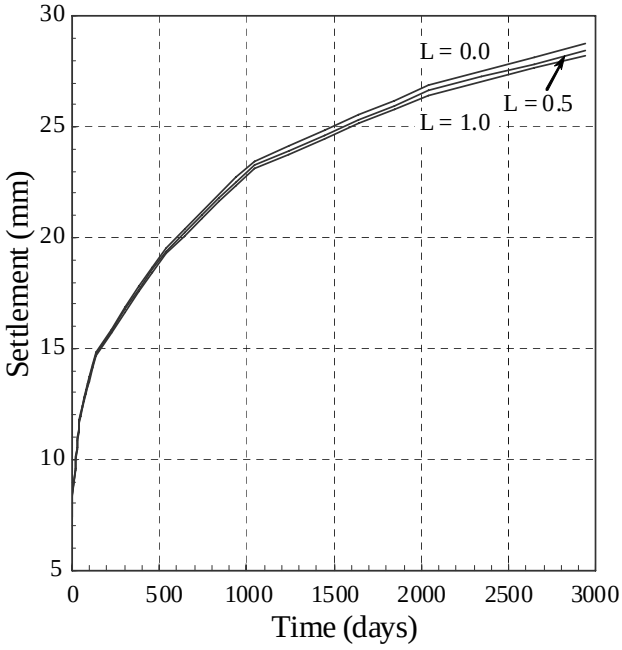

Figure 7. Settlement behavior of three selected points at the foundation level with time. $L =$ (distance from center point)/1.2 m.

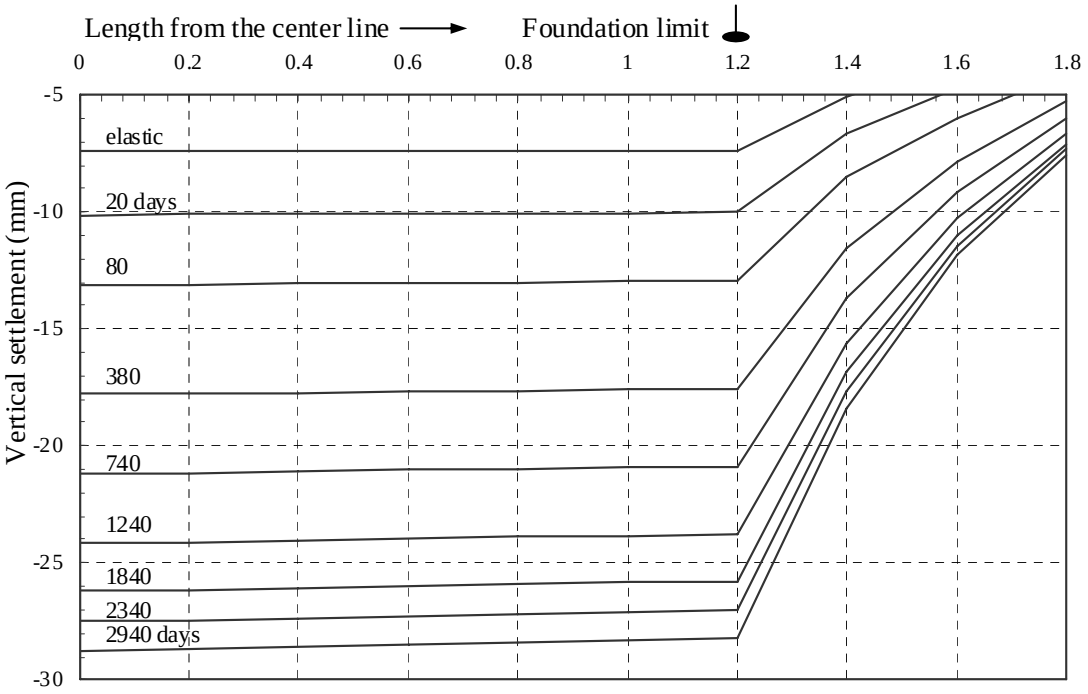

Figure 8. Total settlement behavior at the foundation level with time.

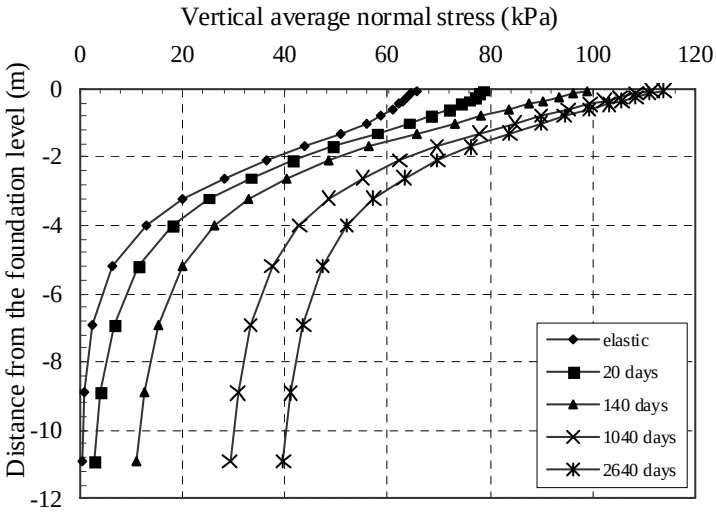

Figure 9. Average normal stress distribution at a distance of 0.1 m from the centerline (underneath the foundation) with time.

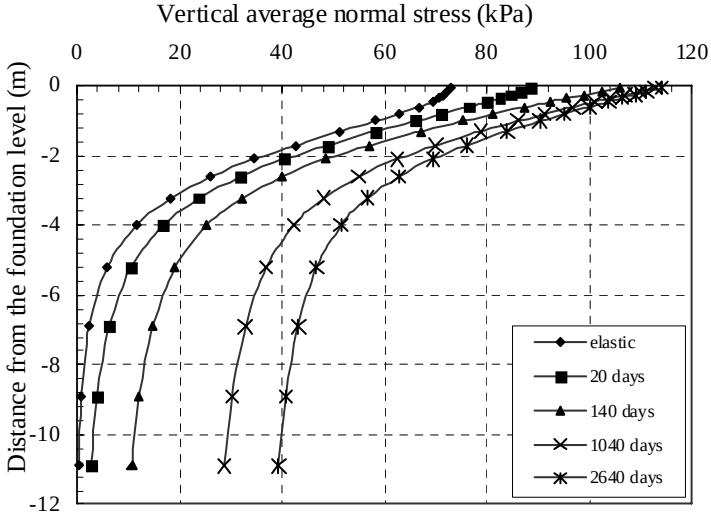

Figure 10. Average normal stress distribution at a distance of 0.5 m from the centerline (underneath the foundation) with time.

The stress distribution at a vertical section outside the foundation width is shown in Figure 12. The time dependent average shear stress distributions in the soil along vertical sections at distances of 0.5 m and 1.1 m away from the centerline are shown in Figures 13 and 14, respectively. A general reduction in average shear stress with time underneath the loaded foundation can be seen (under the ultimate lithostatic state expected, shear stress tend to vanish). Figures 12, 13 and 14 show that the far field effects are insignificant in the general case. A similar trend is shown by the elastic solution indicated on Figures 9, 10 and 11. However, under the loaded patch, the normal vertical stress in the soil medium

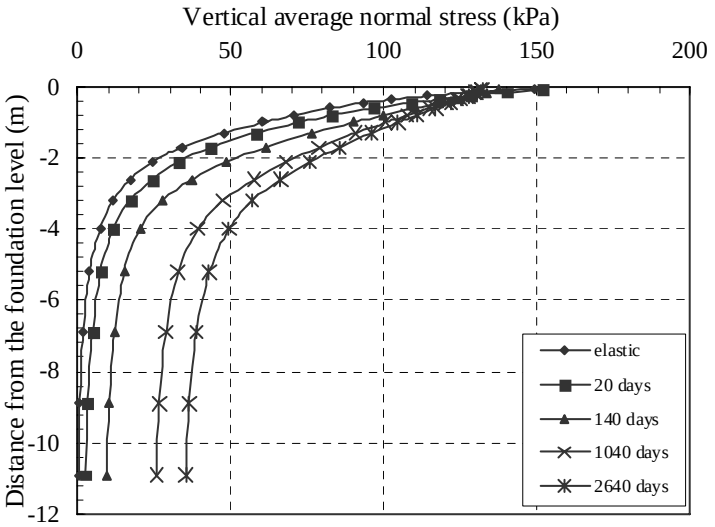

Figure 11. Average normal stress distribution at a distance of 1.1 m from the centerline (underneath the foundation) with time.

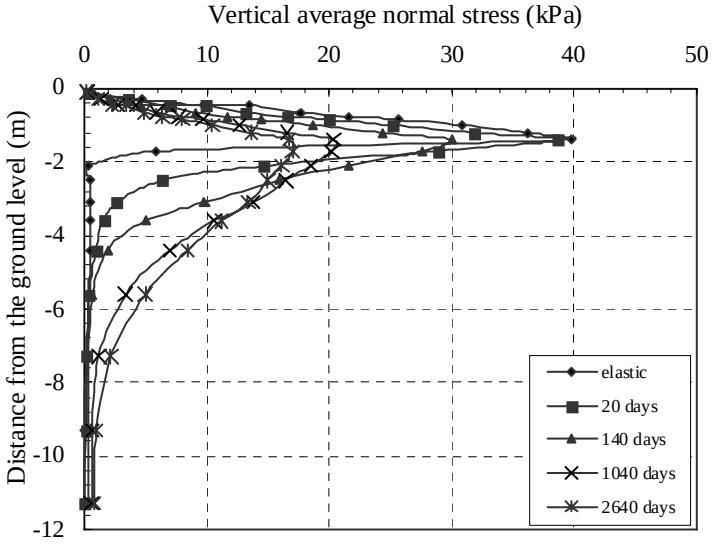

Figure 12. Average normal stress distribution at a distance of 2.1 m from the centerline (outside the foundation) with time.

keeps on increasing with time towards the magnitude of the pressure applied on the footing as a result of the creep of the material, regardless of the depth of the far boundary.

It is noted that the numerical values presented in this analysis are dependent on the selected material parameters which are similar to Haney clay [Vaid and Campanella 1977]. However, the numerically predicted results of the present research compares well with those monitored in the field as reported by Bjerrum [1967]. The numerically predicted results for the soil-structure interaction problem (given by

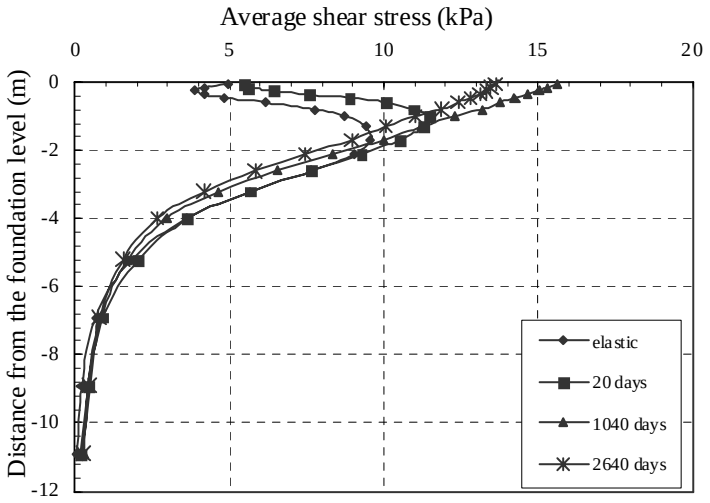

Figure 13. Average shear stress distribution at a distance of 0.5 m from the centerline (underneath the foundation) with time.

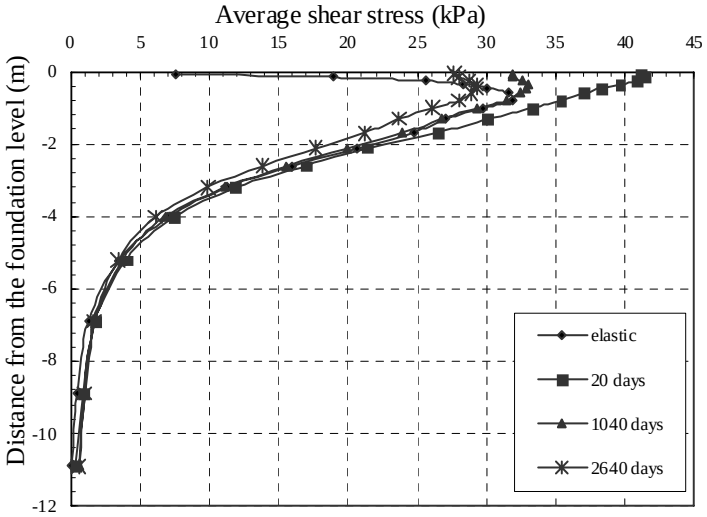

Figure 14. Average shear stress distribution at a distance of 1.1 m from the centerline (underneath the foundation) with time.

Figure 6) are shown in Figure 15, which depicts the time-dependent settlement under the mid-point of the foundation. This time-settlement curve in this last figure shows a behavior qualitatively similar to the monitored behavior of two buildings: Skoger Sparebank Building, Norway and Konnerud Gate 16 Building, Norway, given by Bjerrum [1967], and reproduced approximately in Figure 16.

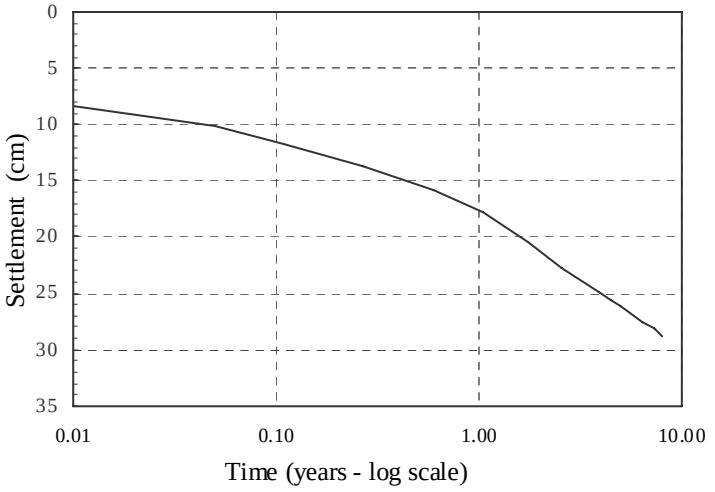

Figure 15. Settlement predicted for the mid-point of foundation depicted in Figure 5 by the finite element analysis.

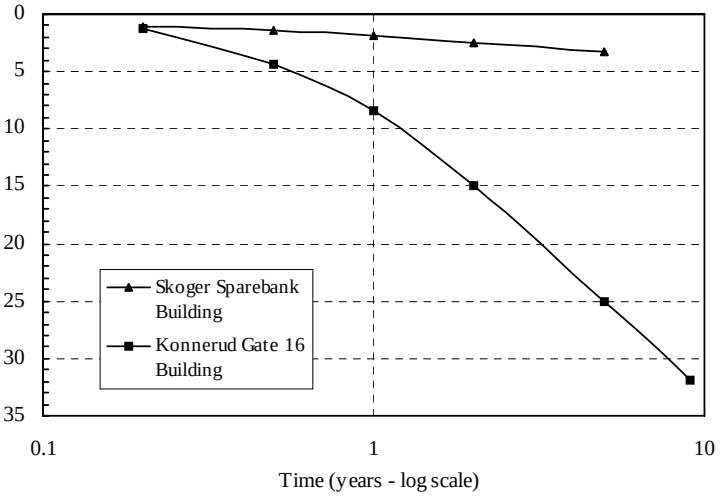

Figure 16. The monitored settlement behavior of the Skoger Sparebank Building, Norway and the Konnerud Gate 16 Building, Norway. From Bjerrum [1967, Figures 23, 25].

7. Conclusion

The modified soil creep model of Bjerrum [1967] has been generalized to multidimensions and implemented in a time-incrementing, iterative, nonlinear finite element code. Analyses were conducted for two cases of a loaded strip footing placed on a clay stratum, under the assumption of simplified plane strain conditions. The sensitivity of settlement predicted by the model to various material parameters is demonstrated. The model predicts that delayed (creep) settlement can be several times the instant (elastic) settlement. The vertical normal stresses under the loaded foundations increase with time towards the

applied vertical pressure magnitude and the shear stress under the loaded foundation decreases with time. This predicted behavior is in confirmation with the tendency of a creeping material to reach a lithostatic state of stress in the long term. The predicted numerical values, while dependent on the selected magnitudes of material parameters, compare qualitatively with reported field data given by Bjerrum. Due to the complications of nonlinear relationships involved in the model, the numerical algorithm experiences some difficulties if arbitrary material parameters are selected. The developed model can be extended by incorporating nonlinear elasticity for elastic strains which was not considered in the present study. But it was seen to function and yield results that capture the essential trends shown by test data for valid material parameters. The computer code developed here, when further developed and verified with field data, would be a useful research tool for estimating settlements in structures founded on soils exhibiting creep.

Acknowledgments

The authors extend their gratitude to the Science and Technology Personnel Development Project of the Ministry of Science and Technology, Sri Lanka, and the Asian Development Bank, who funded this research program. This work was carried out while Madurapperuma was at the Department of Civil Engineering, University of Moratuwa, Sri Lanka.

References

[Adachi and Oka 1982] T. Adachi and F. Oka, "Constitutive equation for normally consolidated clays based on elasto-viscoplasticity", *Soils Found.* **22** (1982), 57–70.

[Adachi and Okano 1974] T. Adachi and F. Okano, "A constitutive equation for normally consolidated clay", *Soils Found.* **14** (1974), 55–73.

[Balasubramaniam and Brenner 1981] A. S. Balasubramaniam and R. P. Brenner, "Consolidation and settlement of soft clay", pp. 480–560 in *Soft clay engineering*, edited by E. W. Brand and R. P. Brenner, Elsevier, New York, 1981.

[Bjerrum 1967] L. Bjerrum, "Engineering geology of Norwegian normally consolidated marine clays as related to settlements of buildings", *Géotechnique* **17** (1967), 81–118.

[Borja and Kavazvjian 1985] R. I. Borja and E. Kavazvjian, "A constitutive model for the σ-ε-t behavior of wet clays", *Géotechnique* **35** (1985), 283–298.

[Brinkgreve 2002] R. B. J. Brinkgreve, *PLAXIS finite element code for soil and rock analyses: user manual*, Balkema, Rotterdam, 2002.

[Butterfield 1979] R. Butterfield, "A natural compression law for soils (an advance on e–log p')", *Géotechnique* **29** (1979), 469–480.

[Garlanger 1972] J. E. Garlanger, "The consolidation of soils exhibiting creep under constant effective stress", *Géotechnique* **22** (1972), 71–78.

[Iizuka and Ohta 1987] A. Iizuka and H. Ohta, "A determination procedure of input parameters in elasto-viscoplastic finite element analysis", *Soils Found.* **27** (1987), 71–87.

[Janbu 1969] N. Janbu, "The resistance concept applied to soils", pp. 191–196 in *Proceedings of the 7th ICSMFE* (Mexico City, 1969), vol. 1, Sociedad Mexicana de Mecánica de Suelos, Mexico City, 1969.

[Puswewala et al. 1992] U. G. A. Puswewala, R. K. N. D. Rajapakse, L. Domaschuk, and R. P. Lach, "Finite element modelling of pressuremeter tests and footings on frozen soils", *Int. J. Numer. Anal. Methods Geomech.* **16**:5 (1992), 351–375.

[Roscoe and Burland 1968] K. H. Roscoe and J. B. Burland, "On the generalized stress-strain behavior of 'wet' clay", pp. 535–609 in *Engineering plasticity*, edited by J. Heyman and F. A. Leckie, Cambridge, Cambridge, 1968.

[Stolle et al. 1997] D. F. E. Stolle, P. G. Bonnier, and P. A. Vermeer, "A soft soil model and experiences with two integration schemes", pp. 123–128 in *Numerical models in geomechanics, NUMOG VI: Proceedings of the 6th International Symposium on Numerical Models in Geomechanics* (Montréal, 1997), edited by S. Pietruszczak and G. N. Pande, Balkema, Rotterdam, 1997.

[Terzaghi 1931] K. Terzaghi, "The static rigidity of plastic clays", *J. Rheol.* **2**:3 (1931), 253–262.

[Vaid and Campanella 1977] Y. Vaid and R. G. Campanella, "Time-dependent behavior of undisturbed clay", *J. Geotech. Eng.* (*ASCE*) **103**:7 (1977), 693–709.

[Vermeer and Neher 1999] P. A. Vermeer and H. P. Neher, "A soft soil model that accounts for creep", pp. 249–261 in *Beyond 2000 in computational geotechnics: 10 years of PLAXIS International* (Amsterdam, 1999), edited by R. B. J. Brinkgreve, Balkema, Rotterdam, 1999.

[Vermeer et al. 1998] P. A. Vermeer, D. F. E. Stolle, and P. G. Bonnier, "From the classical theory of secondary compression to modern creep analysis", pp. 2469–2478 in *Computer methods and advances in geomechanics: proceedings of the Ninth International Conference on Computer Methods and Advances in Geomechanics* (Wuhan, 1997), vol. 4, edited by J.-X. Yuan, Balkema, Rotterdam, 1998.

[Wheeler et al. 2003] S. J. Wheeler, M. Cudny, H. Neher, and C. Wiltafsky, "Some developments in constitutive modeling of soft clays", pp. 3–22 in *International Workshop on Geotechnics of Soft Soils: theory and practice* (Noordwijkerhout, 2003), edited by P. A. Vermeer et al., VGE, Verlag Glückauf, Essen, 2003.

Received 30 May 2007. Revised 18 Nov 2008. Accepted 20 Nov 2008.

M. A. K. M. MADURAPPERUMA: ma.k.aa@m.titech.ac.jp
Department of Civil Engineering, Tokyo Institute of Technology, M-19, 2-12-1, O-okayama, Meguro-ku, Tokyo 152-8552, Japan
http://www.cv.titech.ac.jp/~anil.lab/

U. G. A. PUSWEWALA: head@earth.mrt.ac.lk
Department of Civil Engineering, University of Moratuwa, Katubedda, Moratuwa, Western Province, Sri Lanka
http://www.civil.mrt.ac.lk/